

Title

A High-Order, Time-Dependent, Response Matrix Method for Reactor Kinetics

Author

Jeremy A. Roberts, Ph.D.

Affiliation

Department of Mechanical and Nuclear Engineering, Kansas State University

Address

3002 Rathbone Hall, Manhattan, KS 66506

Email

jaroberts@ksu.edu

Total Number of Pages

26

Total Number of Figures

5

Total Number of Tables

2

A High-Order, Time-Dependent, Response Matrix Method for Reactor Kinetics

Jeremy A. Roberts

Department of Mechanical and Nuclear Engineering, Kansas State University

Abstract

A high-order, transient transport method based on the response matrix formalism is developed for application to reactor kinetics problems. The method combines recent advances in both static and transient response matrix methods with an explicit response-based treatment of delayed neutron precursors first proposed in the 1970s. In addition, an orthogonal basis for the time variable based on point kinetics is proposed as an alternative to a strictly polynomial basis. The method is demonstrated on infinite medium problems, the results of which show that the method can be successfully applied to reactor kinetics problems with and without precursors.

Keywords

time-dependent transport theory; response matrix method; reactor kinetics

I. INTRODUCTION

In a recent article,¹ Pounders and Rahnema presented the development of a time-dependent, incident flux expansion method based on expansions of the space, angle, and time variables in orthogonal polynomials. Their work extends previous work on the steady-state COarsh MESH Transport (COMET) method from the same group, although similar response matrix methods (RMMs) were developed in the 1970s^{2,3} and continue to be studied by a variety of groups around the world.^{4,5} A survey of the RMM literature can be found in Ref. 5.

The transient method proposed by Pounders and Rahnema is closely related to (and can be considered a generalization of) a method published by Sicilian and Pryor⁶ nearly forty years ago. The methods differ in their specific spatial, angular, and temporal discretization; for example, the COMET approach is based on polynomial representations of all variables, while the approach of Sicilian and Pryor is limited to low-order representations, e.g., linear in angle and time, and segmented in space. However, this older method explicitly treated precursors, which was also suggested (but not developed) by Pounders and Rahnema in their preliminary work.⁷

In this note, the relationship between the methods is demonstrated, and the high-order method of Pounders and Rahnema¹ is extended to include an explicit treatment of delayed neutron precursors by following the approach of Sicilian and Pryor.⁶ Section II provides a review of the methods and sets the notation to be used throughout. Section III describes how delayed neutron precursors can be treated as a separate response quantity (like nodal fluxes and boundary currents), while Section IV provides preliminary results based on two infinite medium problems. Finally, Section V provides a discussion of potential implementation issues and other concluding remarks.

II. TIME-DEPENDENT RESPONSE MATRIX METHODS

Response matrix methods are based on the spatial partitioning of a global domain into independent nodes linked together by approximate boundary conditions. The boundary currents and volume fluxes are projected onto a finite, orthogonal basis, and the coefficients of the resulting expansion become the unknowns. In this section, the time-dependent, response matrix method of Pounders and Rahnema¹ is summarized. Although the original presentation is followed, a slightly less formal notation is adopted in places for brevity, and some of the notation used by Sicilian and Pryor⁶ is introduced for increased clarity.

A. The Time-Dependent Transport Equation

Consider the time-dependent transport equation (TDTE), which, in operator form, can be written

$$\frac{1}{v} \frac{\partial \psi}{\partial t} + \mathcal{H}\psi(\mathbf{r}, \mathbf{v}, t) = q_{\text{ext}}(\mathbf{r}, \mathbf{v}, t), \quad (1)$$

where ψ is the angular flux, \mathbf{r} is the spatial coordinate, \mathbf{v} is the velocity vector (and $v = |\mathbf{v}|$), \mathcal{H} represents all transport processes, and q_{ext} is an external source.

Suppose the global problem of Eq. (1) is defined over a spatial volume V which can be decomposed into N disjoint, nodal subvolumes V_n that satisfy $V = V_1 \cup V_2 \cup \dots \cup V_N$. Then an equivalent transport problem for the n th node is

$$\frac{1}{v} \frac{\partial \psi}{\partial t} + \mathcal{H}\psi(\mathbf{r}_n, \mathbf{v}, t) = q(\mathbf{r}_n, \mathbf{v}, t), \quad (2)$$

subject to the initial condition

$$\psi(\mathbf{r}_n, \mathbf{v}, 0) = \psi_{\text{global}}(\mathbf{r}_n, \mathbf{v}, 0), \quad (3)$$

and the incident current conditions

$$j(\mathbf{r}_{n_i}, \mathbf{v}, t) = j_{\text{global}}(\mathbf{r}_{n_i}, \mathbf{v}, t), \quad \mathbf{v} \cdot \mathbf{n}_i < 0, \quad (4)$$

where $j(\mathbf{r}_{n_i}, \mathbf{v}, t)$ is the angular current through a nodal surface i with outward normal \mathbf{n}_i . Ponders and Rahnema showed that the initial and boundary conditions can be represented as sources, leading to the modified local TDTE,

$$\begin{aligned} \frac{1}{v} \frac{\partial \psi}{\partial t} + \mathcal{H}\psi(\mathbf{r}_n, \mathbf{v}, t) &= \overbrace{q_{\text{ext}}(\mathbf{r}_n, \mathbf{v}, t)}^{\text{external source}} \\ &+ \overbrace{\sum_{i=1}^I j(\mathbf{r}_{n_i}, \mathbf{v}, t) H(-\mathbf{v} \cdot \mathbf{n}_i) \delta(\mathbf{r}_{n_i} - \mathbf{r}_n)}^{\text{boundary conditions}} \\ &+ \overbrace{v^{-1} \psi(\mathbf{r}_n, \mathbf{v}, 0) \delta(t)}^{\text{initial condition}}, \end{aligned} \quad (5)$$

where $\delta(x)$ is the Dirac- δ function, $H(x)$ is the Heaviside step function, and I is the number of nodal surfaces. Because both q_{ext} and $v^{-1}\psi$ represent volumetric sources, they are combined into one effective volume source q for brevity.

Because the transport equation is linear, the general solution for an arbitrary source q can be defined by the convolution of the source term with the appropriate kernel, assuming that the system properties are time-invariant. By adapting the notation of Sicilian and Pryor,⁶ the local flux can be expressed as

$$\begin{aligned} \psi(\boldsymbol{\rho}_n) &= \int_0^t dt' \left[\int d^3 r' \int d^3 v' R_{ss}(\boldsymbol{\rho}'_n, \boldsymbol{\rho}_n) q(\boldsymbol{\rho}'_n) + \right. \\ &\left. \sum_{i=1}^I \left(\int_{\mathbf{r}'_n \in \mathbf{r}_{n_i}} d^2 r' \int_{\mathbf{n}_s \cdot \mathbf{v}' < 0} d^3 v' R_{cs}(\boldsymbol{\rho}'_n, \boldsymbol{\rho}_n) j(\boldsymbol{\rho}'_n) \right) \right], \end{aligned} \quad (6)$$

where $(\boldsymbol{\rho}) \equiv (\mathbf{r}, \mathbf{v}, t)$. The outgoing angular currents can be similarly expressed

as

$$j^+(\boldsymbol{\rho}_{n_i}) = \int_0^t dt' \left[\int d^3r' \int d^3v' R_{sc}(\boldsymbol{\rho}'_n, \boldsymbol{\rho}_n) q(\boldsymbol{\rho}'_n) + \sum_{i=1}^I \int_{\mathbf{r}'_n \in \mathbf{r}_{n_i}} d^2r' \int_{\mathbf{n}_s \bullet \mathbf{v}' < 0} d^3v' R_{cc}(\boldsymbol{\rho}'_n, \boldsymbol{\rho}_n) j(\boldsymbol{\rho}'_n) \right]. \quad (7)$$

The source-specific kernels (called “response functions”) R_{ss} , R_{cs} , R_{sc} , and R_{cc} represent the angular flux (or outgoing current) at $\boldsymbol{\rho}$ due to a unit point source (or incident current) at $\boldsymbol{\rho}'$. For example, $R_{sc}(\boldsymbol{\rho}', \boldsymbol{\rho})$ is the outgoing angular current at $\boldsymbol{\rho}$ due to a unit point source at $\boldsymbol{\rho}'$, which is suggested by the subscripts s (volume source) to c (current response).

B. Projection onto a Space and Velocity Subspace

Before proceeding to a temporal discretization, the spatial and velocity dependence are first eliminated by projecting the local currents and fluxes onto a finite subspace represented by an orthogonal basis. Ponders and Rahnema employed a basis constructed with tensor products of polynomials in space and angle.¹ However, if the underlying transport approximation consists of discrete variables, then discrete polynomials can be used.^{5,8} Other subspace bases are possible, including the segmentation of the spatial domain (surface or volume) into regions in which the spatial dependence of the flux or current is assumed to be constant, as employed by Sicilian and Pryor.⁶ Segmentation in angle is also possible.⁴ Most previous work on RMMs used multigroup transport methods with a complete basis of Kronecker- δ functions to represent exactly the energy group-dependence of response functions. However, alternative discrete bases have recently been developed to provide accurate approximations with many fewer degrees of freedom than a full multigroup approach.⁹

Let a finite basis be constructed with a set of functions, $P^m(\mathbf{r}, \mathbf{v})$, $m = 0, 1, \dots, M$,

which are orthonormal over some domain of interest (i.e., either a volume or a surface). Then the volume source q can be approximated as

$$q(\mathbf{r}_n, \mathbf{v}, t) \approx \sum_{m=0}^M q_n^m(t) P_s^m(\mathbf{r}_n, \mathbf{v}), \quad (8)$$

where

$$q_n^m(t) = \int d^3 r' \int d^3 v' q(\mathbf{r}_n, \mathbf{v}, t) P_s^m(\mathbf{r}_n, \mathbf{v}), \quad (9)$$

and the s subscript denotes a (volumetric) source basis. The angular currents can similarly be approximated as

$$j^\pm(\mathbf{r}_{n_i}, \mathbf{v}, t) \approx \sum_{l=0}^L j_{n_i}^{\pm l}(t) P_c^l(\mathbf{r}_{n_i}, \mathbf{v}), \quad \mathbf{n}_i \cdot \mathbf{v} \gtrless 0, \quad (10)$$

where

$$j_{n_i}^{\pm l}(t) = \int_{\mathbf{r}'_n \in \mathbf{r}_{n_i}} d^2 r' \int_{\mathbf{n}_i \cdot \mathbf{v} \gtrless 0} d^3 v' j(\mathbf{r}_{n_i}, \mathbf{v}, t) P_c^l(\mathbf{r}_{n_i}, \mathbf{v}), \quad (11)$$

and the c subscript denotes a (surface) current basis.

The substitution of Eqs. (8) and (10) into Eq. (6) yields

$$\psi(\boldsymbol{\rho}_n) \approx \int_0^t dt' \left[\sum_{m=0}^M q_n^m(t') \langle R_{ss}, P_s^m \rangle + \sum_{i=1}^I \sum_{l=0}^L j_{n_i}^{-l}(t') \langle R_{cs}, P_c^l \rangle \right], \quad (12)$$

where variables have been suppressed and $\langle \cdot \rangle$ indicates the appropriate space and velocity integration. Separate indices (i.e., m and l) are used for the surface and volume terms to indicate that the bases and the number of terms used can be different.

After multiplying Eq. (12) by $P_s^{m'}$ and integrating the result over space and

velocity, a set of flux moments is defined as

$$\begin{aligned} \psi_n^{m'}(t) \approx & \int_0^t dt' \left[\sum_{m=0}^M q_n^m(t') \langle \langle R_{ss}, P_s^m \rangle, P_s^{m'} \rangle \right. \\ & \left. + \sum_{i=1}^I \sum_{l=0}^L j_{n_i}^{-l}(t') \langle \langle R_{cs}, P_c^l \rangle, P_s^{m'} \rangle \right], \end{aligned} \quad (13)$$

or

$$\begin{aligned} \psi_n^{m'}(t) \approx & \int_0^t dt' \left[\sum_{m=0}^M q_n^m(t') R_{ss}^{mm'}(t-t') \right. \\ & \left. + \sum_{i=1}^I \sum_{l=0}^L j_{n_i}^{-l}(t') R_{cs}^{lm'}(t-t') \right], \end{aligned} \quad (14)$$

where the response function moments (e.g., $R_{ss}^{mm'}$) remain functions of time. The outgoing angular currents can also be projected to yield the moments

$$\begin{aligned} j_n^{+l'}(t) \approx & \int_0^t dt' \left[\sum_{m=0}^M q_n^m(t') R_{sc}^{m'l'}(t-t') \right. \\ & \left. + \sum_{i=1}^I \sum_{l=0}^L j_{n_i}^{-l}(t') R_{cc}^{ll'}(t-t') \right]. \end{aligned} \quad (15)$$

The formalism represented by Eqs. (14) and (15), without specifying the space and velocity bases used for projection, is equivalent to that of Pounders and Rahnema (e.g., Eqs. (24)–(26) of Ref. 1) and can be viewed as a generalization of the method of Sicilian and Pryor (e.g., Eqs. (4) and (5) of Ref. 6).

C. Projection onto a Temporal Subspace

To treat the time dependence of the responses, a similar projection technique can be used.¹ Consider the generic time integral

$$y(t) = \int_0^t j(t') R(t-t') dt', \quad (16)$$

typical of the flux and moment equations derived above. With the use of a set of functions $P^k(t)$, $k = 0, 1 \dots, K$, that are orthonormal over the time domain of interest, the function $j(t)$ can be approximated as

$$j(t) \approx \sum_{k=0}^K j^k P^k(t), \quad (17)$$

where

$$j^k = \int_0^t j^k P^k(t') dt', \quad (18)$$

and the function $R(t)$ can be approximated as

$$R(t) \approx \sum_{k=0}^K R^k P^k(t), \quad (19)$$

where

$$R^k = \int_0^T R(t) P^k(t) dt. \quad (20)$$

Then the function $y(t)$ can be approximated as

$$y(t) \approx \sum_{k=0}^K \sum_{k'=0}^{K'} j^k R^{k'} \int_0^t P^k(t) P^{k'}(t-t') dt'. \quad (21)$$

However, the expansion of $R(t)$ may be unnecessary. If $R(t)$ can be explicitly evaluated, then it can be directly used in the convolution integral, so that

$$y(t) \approx \sum_{k=0}^K j^k \int_0^t P^k(t) R(t-t') dt'. \quad (22)$$

This direct substitution can be quite important. In scoping studies, response moments based on Eq. (21) were found to differ from (the more accurate) moments of Eq. (22) by as much as 50%.

The time-dependent flux, current, and response function moments of Eqs. (14)–(15) can be projected onto a temporal basis, just as was done to treat the space and

velocity dependence. First, the moments of ψ , j , and q are expanded in the temporal basis, following Eqs. (17) and (18), and the expansions are substituted into Eqs. (14) and (15). After multiplying the result by $P^{k'}$ and integrating over time $t \in [0, T]$, the flux and current moments are defined

$$\begin{aligned} \psi_n^{m'k'} &= \sum_{m=0}^M \sum_{k=0}^K q^{mk} R_{ss}^{mm'kk'} \\ &+ \sum_{i=1}^I \sum_{l=0}^L \sum_{k=0}^K j_{n_i}^{-lk} R_{cs}^{lm'kk'} , \end{aligned} \quad (23)$$

and

$$\begin{aligned} j_{n_i}^{+lk'} &= \sum_{m=0}^M \sum_{k=0}^K q^{mk} R_{sc}^{ml'kk'} \\ &+ \sum_{i=1}^I \sum_{l=0}^L \sum_{k=0}^K j_{n_i}^{-lk} R_{cc}^{ll'kk'} , \end{aligned} \quad (24)$$

where, for example,

$$R_{ss}^{mm'kk'} = \int_0^T dt \int_0^t P^k(t') P^{k'}(t) R_{ss}^{mm'}(t-t') dt' . \quad (25)$$

For the specific case of an initial condition, the time-dependent source moments are

$$q^m(t) = \psi_0^m v^{-1} \delta(t) . \quad (26)$$

The contribution to a flux moment from the initial condition can be directly computed as

$$\begin{aligned} \psi_{IC}^{mk} &= \int_0^T dt \int_0^t \psi_0^m v^{-1} \delta(t') R_{ss}^{mm'}(t-t') dt' \\ &= \psi_0^m v^{-1} \int_0^T R_{ss}^{mm'}(t) dt \equiv \psi_0^m R_{ss0}^{mm'} . \end{aligned} \quad (27)$$

Equation (23), (24), and (27) can be represented as nodal response matrix

equations, i.e.,

$$\boldsymbol{\psi}_n = \mathbf{R}_n^{ss} \mathbf{q}_n + \mathbf{R}_n^{cs} \mathbf{j}_n^- + \mathbf{R}_n^{ss0} \boldsymbol{\psi}_{0n}, \quad (28)$$

and

$$\mathbf{j}_n^+ = \mathbf{R}_n^{sc} \mathbf{q}_n + \mathbf{R}_n^{cc} \mathbf{j}_n^-, \quad (29)$$

where $\boldsymbol{\psi}_n$, \mathbf{j}_n^\pm , and \mathbf{q}_n are vectors of nodal moments, and the \mathbf{R}_n 's are matrices of nodal response function moments. Response matrix equations for the entire spatial domain can then be written as

$$\begin{aligned} \boldsymbol{\psi} &= \mathbf{R}^{ss} \mathbf{q} + \mathbf{R}^{cs} \mathbf{j}^- + \mathbf{R}^{ss0} \boldsymbol{\psi}_0 \\ \mathbf{j}^+ &= \mathbf{R}^{sc} \mathbf{q} + \mathbf{R}^{cc} \mathbf{j}^-. \end{aligned} \quad (30)$$

By redirecting outgoing currents from one node as incident currents to another via $\mathbf{j}^- = \mathbf{M} \mathbf{j}^+$, where \mathbf{M} is a matrix that represents the global geometry and boundary conditions, the global equations become

$$\begin{aligned} \boldsymbol{\psi} &= \mathbf{R}^{ss} \mathbf{q} + \mathbf{R}^{cs} \mathbf{j}^- + \mathbf{R}^{ss0} \boldsymbol{\psi}_0 \\ \mathbf{j}^- &= \mathbf{M} \mathbf{R}^{sc} \mathbf{q} + \mathbf{M} \mathbf{R}^{cc} \mathbf{j}^-. \end{aligned} \quad (31)$$

After computing the flux moments $\boldsymbol{\psi}$ the flux can be evaluated at the end time T , and the result can be used as the initial condition for a subsequent time interval with possibly updated responses.

D. Selection of Temporal Subspaces

Various bases can be employed for the temporal projection. Pounders and Rahnema¹ used the Legendre polynomials, scaled and translated to be orthogonal over a finite time interval $t \in [0, T]$. In addition, they computed all response function moments with Monte Carlo.

In a simpler approximation, Sicilian and Pryor⁶ defined a set of discrete times $t_0 = 0, t_1, \dots, t_N = T$ between which the current was assumed to vary linearly

in time and the volume terms were assumed to be constant in time. They used a simple modification of static (i.e., time-independent) responses to approximate first-order temporal moments, although they noted the error introduced to the solution was small compared to a solution using first-order moments computed directly from Monte Carlo.

Another possibility for treating the time variable is to incorporate some aspect of the anticipated temporal behavior, similar to specialized space, angle, and energy bases proposed that capture some physics.^{9,10} For reactor point kinetics problems, the time-dependence of the neutron population is exponential with time constants related to the roots of the in-hour equation. If the appropriate point kinetics parameters can be estimated for the system *a priori*, then a good temporal basis may include a set of exponential functions made orthogonal by the Gram-Schmidt (or similar) process. One instance of this approach is studied in Section IV, in which approximate prompt and delayed neutron time constants are used to define two exponential functions that are combined with polynomials as a temporal basis.

III. RESPONSE-BASED PRECURSOR CONCENTRATIONS

In the original work of Sicilian and Pryor, delayed neutron precursor concentrations were explicitly treated in place of the volumetric fluxes and were assumed to represent an isotropic source uniformly distributed in space within a node.⁶ However, a similar approach can be taken within the more general framework described in Section II to define a general, high-order treatment of the precursor concentrations.

The TDTE, including precursors, is

$$\begin{aligned} \frac{1}{v} \frac{\partial \psi}{\partial t} + \mathcal{H}\psi(\mathbf{r}, \mathbf{v}, t) &= q(\mathbf{r}, \mathbf{v}, t) \\ &+ \frac{1}{4\pi} \sum_{i=1}^N \lambda_i c_i(\mathbf{r}, t) \chi(\mathbf{r}, \mathbf{v}), \end{aligned} \tag{32}$$

where the concentration of the i th precursor satisfies

$$\begin{aligned} \frac{\partial c_i}{\partial t} = & -\lambda_i c_i(\mathbf{r}, t) \\ & + \beta_i(\mathbf{r}) \int \nu \Sigma_f(\mathbf{r}, \mathbf{v}) \psi(\mathbf{r}, \mathbf{v}, t) d^3v, \quad i = 1 \dots N. \end{aligned} \quad (33)$$

The production of prompt neutrons from fission is incorporated implicitly in the operator \mathcal{H} . Although the precursors can also be treated implicitly,¹¹ the resulting response functions have long “tails” with time constants close to those of the precursors, which leads to numerical difficulties resolved only by rather limiting approximations.⁶ However, the precursors represent a source that can be handled separately from the flux as a new response quantity. The general solution to the i th precursor equation is

$$\begin{aligned} c_i(\mathbf{r}, t) = & c_{0i}(\mathbf{r}) e^{-\lambda_i t} + \\ & \int_0^t dt' \beta_i(\mathbf{r}) \int \nu \Sigma_f(\mathbf{r}, \mathbf{v}) \psi(\mathbf{r}, \mathbf{v}, t') e^{-\lambda_i(t-t')} d^3v, \end{aligned} \quad (34)$$

where the nodal index n has been suppressed. To use the subspace projection techniques of Section II, the approximate angular flux is substituted into Eq. (34), which leads to

$$\begin{aligned} c_i(\mathbf{r}, t) \approx & c_{i0}(\mathbf{r}) e^{-\lambda_i t} \\ & + \int_0^t dt' \beta_i(\mathbf{r}) \int \nu \Sigma_f(\mathbf{r}, \mathbf{v}) \\ & \times \sum_m \sum_k \psi^{mk} P_s^m(\mathbf{r}, \mathbf{v}) P^k(t) e^{-\lambda_i(t-t')} d^3v. \end{aligned} \quad (35)$$

By multiplying both sides of Eq. (35) by $P^{j'}(\mathbf{r}) P^{k'}(t)$ and integrating the result

over space and time, the precursor concentration moments are defined as

$$\begin{aligned}
c_i^{j'k'} &= \int P^{j'}(\mathbf{r}) c_{i0}(\mathbf{r}) d^3r \int_0^T P^{k'}(t) e^{-\lambda_i t} dt + \\
&\sum_m \sum_k \psi^{mk} \left(\int_0^T dt \int_0^t dt' P^{k'}(t) P^k(t') e^{-\lambda_i(t-t')} \right. \\
&\times \left. \int d^3r \beta_i(\mathbf{r}) P^{j'}(\mathbf{r}) \int \nu_{\Sigma_f}(\mathbf{r}, \mathbf{v}) P_s^m(\mathbf{r}, \mathbf{v}) d^3v \right),
\end{aligned} \tag{36}$$

or, in response notation,

$$c_i^{j'k'} = c_{i0}^{j'} R_{i0}^{k'} + \sum_m \sum_k R_i^{mj'kk'} \psi^{mk}. \tag{37}$$

The precursor source in the TDTE must also be represented in moment in order to obtain a consistent set of linear equations. For the i th precursor,

$$q_{c_i}(\mathbf{r}, \mathbf{v}, t) = \frac{1}{4\pi} \lambda_i c_i(\mathbf{r}, t) \chi(\mathbf{r}, \mathbf{v}). \tag{38}$$

The substitution of the approximate precursor concentrations into Eq. 38 leads to

$$q_{c_i}(\mathbf{r}, \mathbf{v}, t) = \frac{1}{4\pi} \lambda_i \chi(\mathbf{r}, \mathbf{v}) \sum_j \sum_k c_i^{jk} P^j(\mathbf{r}) P^k(t). \tag{39}$$

Multiplication of Eq. (39) by $P^{k'}(t)$ and integration of the result over time leads to the source moments

$$\begin{aligned}
q_{c_i}^{m'k'} &= \frac{\lambda_i}{4\pi} \sum_j \sum_k c_i^{jk} \left(\int d^3r \int d^3v \int_0^T dt \right. \\
&\times \left. P^{m'}(\mathbf{r}, \mathbf{v}) \chi(\mathbf{r}, \mathbf{v}) P^j(\mathbf{r}) P^{k'}(t) P^k(t) \right),
\end{aligned} \tag{40}$$

or, in response notation,

$$q_{c_i}^{m'k'} = \frac{\lambda_i}{4\pi} \sum_j R^{jm'k'} c_i^{jk}, \tag{41}$$

where the orthogonality of the functions $P^k(t)$ has been employed.

The global response matrix equations, defined by Eq. (31), together with the precursor equations, Eq. (37), and the augmented source, Eq. (41), can be written

$$\begin{aligned}\boldsymbol{\psi} &= \mathbf{R}^{ss}(\mathbf{q} + \mathbf{R}^{sp}\mathbf{c}) + \mathbf{R}^{cs}\mathbf{j}^- + \mathbf{R}^{ss0}\boldsymbol{\psi}_0 \\ \mathbf{j}^- &= \mathbf{MR}^{sc}(\mathbf{q} + \mathbf{R}^{sp}\mathbf{c}) + \mathbf{MR}^{cc}\mathbf{j}^- \\ \mathbf{c} &= \mathbf{R}^{p0}\mathbf{c}_0 + \mathbf{R}^{ps}\boldsymbol{\psi}.\end{aligned}\tag{42}$$

Given the source and initial conditions, the flux and precursor moments can be found directly by solving the linear system.

IV. NUMERICAL RESULTS

As a preliminary test of the high-order, time-dependent response matrix method for reactor kinetics, two infinite, homogeneous medium problems were studied. By isolating only the dependence on time, the accuracy of various temporal approximations can be studied directly. All results were generated using a stand-alone implementation intended for demonstration and not efficiency. The inclusion of other variables and an assessment of computational efficiency is planned for future work.

A. Prompt Supercritical Kinetics without Delayed Neutrons

To verify the method, a one-group, supercritical system ($k_\infty = 1.1$) was studied subject to the constant source

$$Q(n) = \begin{cases} 1 & 0 \leq t \leq T \\ 0 & t > T, \end{cases}\tag{43}$$

for which the resulting flux is

$$\boldsymbol{\psi}(t) = \begin{cases} \frac{1 - e^{-v(\Sigma_t - \Sigma_s - \nu\Sigma_f)t}}{\Sigma_t - \Sigma_s - \nu\Sigma_f} & 0 \leq t \leq T \\ \boldsymbol{\psi}(T)e^{-v(\Sigma_t - \Sigma_s - \nu\Sigma_f)(t-T)} & t > T. \end{cases}\tag{44}$$

The fission cross section is decreased to produce a subcritical system ($k_\infty = 0.9$) at $t = T = 21\bar{t}$, where the neutron lifetime \bar{t} is taken to be¹²

$$\bar{t} = \frac{1}{v\Sigma_a} = \frac{1}{v(\Sigma_t - \Sigma_s)}, \quad (45)$$

after which the flux is followed until $t = 42\bar{t}$. The values used for each parameter are provided in Table I.

TABLE I. PARAMETERS FOR PROMPT SUPERCRITICAL EXAMPLE.

Parameter	Value	
	$0 \leq t < 21\bar{t}$	$21\bar{t} \leq t \leq 42\bar{t}$
Σ_t	1.00	1.00 1/cm
Σ_s	0.50	0.50 1/cm
$\nu\Sigma_f$	0.55	0.45 1/cm
v	2×10^6 cm/s	2×10^6 cm/s

Several temporal approximations based on the Legendre polynomials were studied. In all cases, responses were computed separately for the supercritical and subcritical time intervals because of the different materials in each interval. Each interval was divided into N subintervals within which a Legendre expansion of order M was used to represent the time dependence. The reference flux defined by Eq. (44) and several low-order approximations are shown in Fig. 1. The resulting relative flux errors from several combinations of N and M are provided in Fig. 2, while a map of the average, absolute, relative error is given in Fig. 3.

As has been noted previously,¹ the errors in the flux tend to be greatest near the time interval boundaries, which is a feature common to polynomial approximations in many applications. The sharp drops observed in Fig. 2 correspond to times at which the approximate flux is exact (in this case, at the zeros of the shifted and scaled Legendre polynomials of degree $M + 1$). These drops occur consistently only in the first time interval because all subsequent intervals start

with an inexact flux. For case (1, 1), the flux is, at times, negative and exhibits a large discontinuity at $t = 21\bar{t}$. Finally, Fig. 3 shows that the reduction in the error due to an increased number of subintervals is substantially magnified at higher expansion orders.

B. Delayed Supercritical Kinetics

To test the method with delayed neutrons, a problem similar to that of Section IV-A was studied with a single delayed neutron precursor group defined by $\beta = 0.0075$ and $\lambda = 0.01 \text{ s}^{-1}$. The system is critical for $t < 0$ with $\nu\Sigma_f = 0.5$ and $\psi_0 = 1.0$. At $t = 0$, the absorption cross section is lowered, reflected by a transition to $\Sigma_s = 0.5(1 + 0.99\beta)$, and the result is followed for 1 second. The system contains no external source.

Several temporal discretizations were studied. In addition to the Legendre basis, a basis containing exponential functions was also used. The time dependence of the flux is generally very complicated but frequently can be described accurately by a linear combination of exponential functions with time constants related to the prompt neutron lifetime and the precursor half lives. For the point kinetics equations, the solution is *exactly* a linear combination of appropriate exponentials if the reactivity is constant. For more realistic cases, the dependence on space, angle, and energy leads to a more complicated dependence on time, but if reasonable estimates of point kinetics parameters are available, then a basis that yields accurate, low-order approximations should be possible to construct. For this study, the reactivity *is* constant, and the solution is

$$\begin{aligned}\psi(t) &\approx 97.46063143e^{\omega_1 t} - 96.46063143e^{\omega_2 t} \\ c(t) &\approx 0.37023900e^{\omega_1 t} + 0.00476100e^{\omega_2 t},\end{aligned}\tag{46}$$

where $\omega_1 = 0.97713904 \text{ s}^{-1}$ and $\omega_2 = -75.98713904 \text{ s}^{-1}$.

However, to test the efficacy of close, but not exact, exponential functions, the

following procedure was used. The two characteristic time constants for the test problem are approximated by

$$\omega_p = v[\Sigma_a - \Sigma_f(1 - \beta)] = -75 \text{ s}^{-1} \quad (47)$$

and

$$\omega_d = \frac{\lambda(\Sigma_f/\Sigma_a - 1)}{\beta + 1 - \Sigma_f/\Sigma_a} \approx 3.84466 \text{ s}^{-1}. \quad (48)$$

The corresponding exponential functions $e^{\omega_p t}$ and $e^{\omega_d t}$ were combined with the monomials 1 , t , and t^2 . Together, the functions were used as a temporal basis after being made mutually orthogonal (starting with $e^{\omega_p t}$ and followed by $e^{\omega_d t}$ and the monomials in order).

The reference flux and precursor concentration defined by Eq. (46) and several low-order approximations are shown in Fig. 4. The low-order approximations capture the time-dependence of the flux and precursors well, while higher-order approximations are virtually indistinguishable from the exact solutions. The Legendre expansions are labeled as $P(M, N)$, where M is the order and N is the number of intervals. The exponential basis expansions are labeled as $E(M, N)$, where M is the maximum polynomial degree included with the two exponential functions. The resulting relative flux errors from several bases are shown in Fig. 5, while Table II summarizes the flux and precursor concentration errors for several bases.

The results indicate that the treatment of two distinct time scales represents a more difficult problem than prompt kinetics alone. For example, a 15th order Legendre expansion with three time subintervals is required to reduce the maximum relative flux error to below 1%. The precursor concentration is a much more slowly-varying quantity, which explains why the associated errors are lower than the flux errors for nearly all of the listed expansions. In addition, the exponential bases were found to produce lower flux errors than Legendre bases with the same

TABLE II. SUMMARY OF ABSOLUTE, RELATIVE ERRORS IN THE FLUX AND PRECURSOR CONCENTRATION FOR SEVERAL DIFFERENT EXPANSIONS.

Basis	Flux Relative Error (%)			Precursor Relative Error (%)		
	average	maximum	at $t = 1$	average	maximum	at $t = 1$
P(5,1)	$4.6 \times 10^{+0}$	$5.6 \times 10^{+3}$	$1.8 \times 10^{+0}$	7.2×10^{-2}	4.1×10^{-1}	1.6×10^{-1}
P(5,3)	$1.7 \times 10^{+0}$	$2.3 \times 10^{+3}$	7.3×10^{-2}	6.9×10^{-2}	1.9×10^{-1}	8.0×10^{-2}
P(5,16)	1.2×10^{-2}	$2.2 \times 10^{+1}$	4.2×10^{-4}	4.6×10^{-4}	2.5×10^{-3}	4.2×10^{-4}
P(15,1)	2.6×10^{-1}	$3.2 \times 10^{+2}$	2.7×10^{-1}	2.7×10^{-3}	2.7×10^{-2}	1.0×10^{-2}
P(15,3)	5.8×10^{-4}	8.9×10^{-1}	2.2×10^{-5}	2.2×10^{-5}	9.0×10^{-5}	2.2×10^{-5}
P(15,16)	6.2×10^{-9}	2.4×10^{-7}	1.4×10^{-8}	7.1×10^{-9}	9.8×10^{-8}	4.7×10^{-9}
E(0,1)	$1.0 \times 10^{+1}$	$3.1 \times 10^{+3}$	$1.2 \times 10^{+1}$	$8.5 \times 10^{+0}$	$3.2 \times 10^{+1}$	$1.3 \times 10^{+1}$
E(0,3)	$2.2 \times 10^{+0}$	$2.1 \times 10^{+2}$	$5.3 \times 10^{+0}$	$2.2 \times 10^{+0}$	$5.7 \times 10^{+0}$	$5.7 \times 10^{+0}$
E(1,1)	8.9×10^{-1}	$3.9 \times 10^{+2}$	$1.0 \times 10^{+0}$	7.0×10^{-1}	$3.2 \times 10^{+0}$	$1.2 \times 10^{+0}$
E(1,3)	9.4×10^{-2}	$5.3 \times 10^{+1}$	1.5×10^{-1}	6.2×10^{-2}	1.9×10^{-1}	1.7×10^{-1}
E(2,1)	5.1×10^{-2}	$3.0 \times 10^{+1}$	5.6×10^{-2}	4.3×10^{-2}	2.3×10^{-1}	8.7×10^{-2}
E(2,3)	2.3×10^{-2}	$3.3 \times 10^{+1}$	1.4×10^{-3}	1.1×10^{-3}	6.1×10^{-3}	1.1×10^{-3}

(or, in some cases, a greater) number of basis functions. For example, the $E(2, 1)$ expansion outperformed the $P(15, 1)$ expansion, but for $P(15, N)$, an increase in N led to a much faster reduction in the error than for $E(2, N)$.

V. SUMMARY

A high-order, time-dependent, response matrix method has been developed for application to reactor kinetics problems with delayed neutron precursors. The method is an extension of the work of Pounders and Rahnema¹ and a generalization of the early work by Sicilian and Pryor.⁶ The method was demonstrated on infinite medium problems, and the results show that the method can adequately treat time dependence. For problems with delayed neutron precursors, very high-order polynomial expansions were required to reduce relative, absolute errors to acceptable (sub-1%) values for the flux and precursor concentrations. As an

alternative to a strictly polynomial basis, a basis was implemented that combines polynomials with exponential functions based on point kinetics approximations and led to lower flux errors than a polynomial basis of similar size.

A general purpose, transient response matrix method offers many potential advantages, in theory, but the application of response matrix methods to realistic problems remains challenging due to the enormous number of response functions required. The addition of the time variable and precursor concentrations greatly increases this number. Moreover, the response function formalism developed so far assumes time-independent materials within fixed time steps; hence, the inclusion of temperature feedback effects, which result in time-varying materials, would lead to an even more complicated task. For response matrix methods to be applicable to steady-state or transient problems of interest, much work remains to be done to reduce the number of response functions necessary for sufficient accuracy. This future work should also include efforts to parameterize the response function dependence on various phase space variables and to deploy response matrix methods on leadership-class, parallel architectures.

ACKNOWLEDGEMENTS

The author would like to thank Professor J. K. Shultis and Professor B. Ganapol for several helpful suggestions to improve the clarity of this note.

REFERENCES

- [1] J. POUNDERS and F. RAHNEMA, “A Coarse-Mesh Method for the Time-Dependent Transport Equation,” *Nuclear Science and Engineering*, **176**, 3, 273 (2014).
- [2] R. PRYOR, “Recent Developments in the Response Matrix Method,” in *Advanced Reactors: Physics, Design, and Economics*, edited by J. KALLFELZ and R. KARAM, Pergamon Press, New York, 1975.
- [3] Z. WEISS and S.-Ö. LINDAHL, “High-Order Response Matrix Equations In Two-Dimensional Geometry,” *Nuclear Science and Engineering*, **58**, 2, 166 (1975).
- [4] K. ISHII, T. HINO, T. MITSUYASU, and M. AOYAMA, “Three-Dimensional Direct Response Matrix Method Using A Monte Carlo Calculation,” *Journal of Nuclear Science and Technology*, **46**, 3, 259 (2009).
- [5] J. ROBERTS and B. FORGET, “Solving Eigenvalue Response Matrix Equations with Nonlinear Techniques,” *Annals of Nuclear Energy*, **69**, 97 (2014).
- [6] J. SICILIAN and R. PRYOR, “TRASCAL: a Two-Dimensional, Multigroup, Response Matrix Kinetics Code,” *Proc. Conference on Computational Methods in Nuclear Engineering*, Charleston, SC, April 15–17, 1975.
- [7] J. POUNDERS and F. RAHNEMA, “A Response-Based Time-Dependent Neutron Transport Method,” *Annals of Nuclear Energy*, **37**, 11, 1595 (2010).
- [8] S. MOSHER and F. RAHNEMA, “The Incident Flux Response Expansion Method for Heterogeneous Coarse Mesh Transport Problems,” *Transport Theory and Statistical Physics*, **35**, 1, 55 (2006).
- [9] R. REED and J. ROBERTS, “Energy Expansion in Response Matrix Methods Using the Karhunen-Loève Transform,” *Transactions of the American Nuclear Society (accepted)*, **110** (2014).
- [10] J. ROBERTS, R. REED, and B. FORGET, “Phase Space Bases for Response Matrix Methods,” *Proc. PHYSOR 2014*, Kyoto, Japan, September 27–October 3, 2014, American Nuclear Society.
- [11] J. SICILIAN, “Response Matrices in Space-Time Reactor Dynamics,” *Nuclear Science Engineering*, **56**, 3, 291 (1975).
- [12] E. LEWIS, *Fundamentals of Nuclear Reactor Physics*, Academic Press (2008).

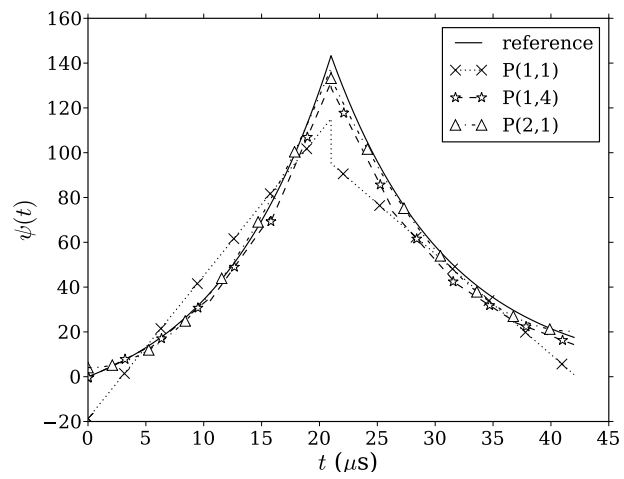


Fig. 1. Reference flux and fluxes computed for low (M, N) values. For higher values, the flux is nearly indistinguishable from the reference solution.

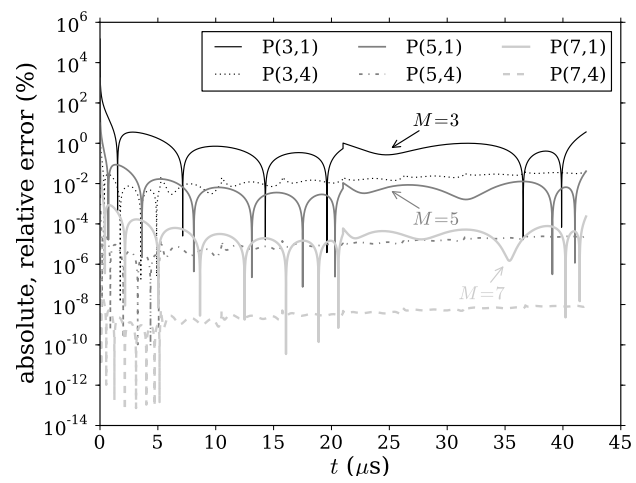


Fig. 2. Absolute, relative error of the flux for various (M, N) values. At $t = 0$, the flux is zero, and because each approximation leads to a nonzero initial flux, the errors near $t = 0$ are very large.

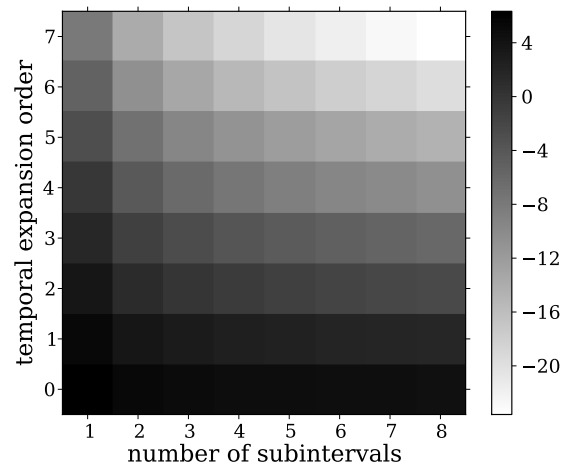


Fig. 3. Natural logarithm of the average, absolute, relative error as a function of the temporal expansion order and the number of subintervals in each temporal interval.

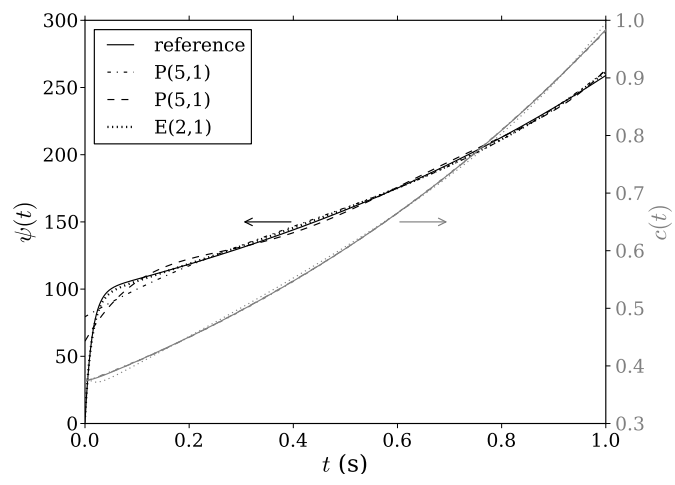


Fig. 4. Reference flux and precursor concentration and various approximations of each.

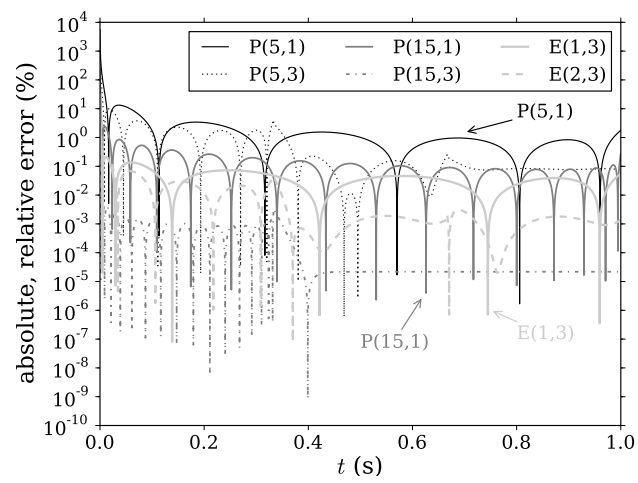


Fig. 5. Absolute, relative error of the flux for various approximations.